

Paramagnetic Cobalt(II) as an NMR Probe of Dendrimer Structure: Mobility and Cooperativity of Dendritic Arms

Jon D. Epperson, Li-June Ming,* Gregory R. Baker, and George R. Newkome*[†]

Contribution from the Department of Chemistry, the Institute for Biomolecular Science, and the Center for Molecular Design & Recognition, University of South Florida, Tampa, Florida 33620-5250

Received March 21, 2001. Revised Manuscript Received July 3, 2001

Abstract: Cobalt(II) has been utilized as an external paramagnetic ¹H NMR probe for the study of the structure of dendrimers that possess specifically located metal recognition sites. The hyperfine-shifted ¹H NMR signals of the Co(II) complexes of several 2,6-diamidopyridine-containing dendrimers have been fully assigned by means of 1D and 2D NMR techniques, including NOE difference, EXSY, COSY, and TOCSY. Temperature-dependent *T*₁ values of the hyperfine-shifted signals were used to conclude that the Co(II)–dendrimer complexes are in the “liquidlike” regime, indicative of a shell-like structure instead of a “dense-core” structure. The presence of sizable cavities within the dendrimers was observed including a loosely packed conformation for the 2,6-diamidopyridino moiety to bind to potential guest molecules. Cooperativity among the dendritic arms in metal binding is also observed, whereby two dendritic arms bind to the metal center at the same time. In the case of dendrimers with the metal binding site located near the surface of the molecule, such binding cooperativity is still observed despite the large degree of freedom of the metal-binding moiety. Cooperativity among the dendritic arms can thus be considered an intrinsic property, which has to be taken into consideration in future design of functional dendrimers for the purpose of specific recognition and catalysis. The hydrodynamic radii of these dendrimers have been determined by means of nuclear Overhauser effect at low temperature. The study offers a method for the study of the dynamics of dendrimers in solution under different conditions and upon ligand binding and recognition. The study also provides a tool for monitoring systematic variation of the metal binding site in different dendrimer frameworks for specific applications, such as catalysis and molecular recognition.

Introduction

Dendrimers are highly branched macromolecules possessing “treelike” structures and are synthesized by repetitively linking molecular building blocks AB_{*n*} (*n* usually 2 or 3) to a central core.¹ Since both the internal and external chemical functionalities of dendrimers can be “tailored” to alter their physical and chemical properties,^{2,3} several potential applications have been found for these polymers, including catalysis,⁴ self-assembly,⁵ and molecular recognition and encapsulation.⁶ For

example, the incorporation of 2,6-diamidopyridino *H*-bonding sites into the internal regions of a polyamido dendrimer (Figure 1) facilitates the selective encapsulation of “guest” molecules such as barbituric acid and 3′-azido-2′,3′-dideoxythymidine (AZT) into the interior of the dendrimer.⁷ Moreover, modification of the dendritic exterior is being explored to produce dendrimers for chromatography additives,⁸ antibody conjugates,⁹ gene therapy,¹⁰ and electrically conducting materials.¹¹

The possibility of entrapping small molecules inside host dendrimers has raised great interest in the structural and chemical characterization of these unique macromolecules;¹² however, detailed structural analyses of dendrimers by means

* Corresponding authors: Dr. Li-June Ming. Tel: (813) 974-2220. Fax: (813)974-1733. E-mail: ming@chuma.cas.usf.edu. Dr. George R. Newkome: Tel: 330-972-6458. E-mail: newkome@uakron.edu; www.dendrimers.com.

[†] Current address: Department of Polymer Science, University of Akron, Akron, OH 44325-4717.

(1) (a) Archut, A.; Vögtle, F. *Chem. Soc. Rev.* **1998**, *27*, 233–240. (b) Narayanan, V. V.; Newkome, G. N. *Topics Curr. Chem.* **1998**, *197*, 19–77. (c) Zeng, F.; Zimmerman, S. C. *Chem. Rev.* **1997**, *97*, 1681–1712. (d) Newkome, G. R.; Moorefield, C. N.; Vögtle, F. *Dendrimers and Dendrons: Concepts, Syntheses, Applications*; Wiley-VCH: Weinheim, Germany, 2001.

(2) Newkome, G. R.; Weis, C. D.; Moorefield, C. N.; Baker, G. R.; Childs, B. J.; Epperson, J. *Angew. Chem., Int. Ed.* **1998**, *37*, 307–310.

(3) Bosman, A. W.; Janssen, H. M.; Meijer, E. W. *Chem. Rev.* **1999**, *99*, 1665–1688.

(4) (a) Brady, P. A.; Levy, E. G. *Chem. Ind.* **1995**, *1/2*, 18. (b) Haggin, J. *Chem. Eng. News* **1995**, *2/6*, 26–27. (c) Tomalia, D. A.; Dvornic, P. R. *Nature* **1994**, *372*, 617–618.

(5) (a) Philip, D.; Stoddart, J. F. *Angew. Chem., Int. Ed. Engl.* **1996**, *35*, 1154–1196. (b) Lawrence, D. S.; Jiang, T.; Levett, M. *Chem. Rev.* **1995**, *95*, 2725–2828. (c) Watanabe, S.; Regen, S. J. *Am. Chem. Soc.* **1994**, *116*, 8855.

(6) (a) Sakthivel, T.; Toth, I.; Florence, A. T. *Int. J. Pharm.* **1999**, *183*, 51–55. (d) Peppas, N. A.; Nagai, T.; Miyajima, M. *Pharm. Techn. Jpn.* **1994**, *10* (6), 611–617.

(7) Newkome, G. R.; Woosley, B. D.; He, E.; Moorefield, C. N.; Guther, R.; Baker, G. H.; Escamillia, J.; Merrill, H.; Luftmann, H. *Chem. Commun.* **1996**, 2737–2738.

(8) (a) Tanaka, N.; Tanigawa, T.; Hosoya, K.; Kimata, K.; Araki, K.; Terabe, A. *Chem. Lett.* **1992**, 959–969. (b) Muijselaar, P. G. H. M.; Classens, H. A.; Cramers, C. A.; Jansen, J. F. G. A.; Meijer, E. W.; de Brabander-van den Berg, E. M. M. *J. High Resol. Chromatogr.* **1995**, *18* (2), 121–123. (c) Dubin, P. L.; Edwards, S. L.; Kaplan, J. I.; Mehta, M. S.; Tomalia, D.; Xia, J. *Anal. Chem.* **1992**, *64* (20), 2344–2347.

(9) (a) Adam, G.; Neuerburg, J.; Spuentrup, E.; Muehler, A.; Scherer, K.; Guenther, R. W. *Magn. Reson. Med.* **1994**, *32* (5), 622–628. (b) Roberts, J. C.; Adams, Y. E.; Tomalia, D.; Mercer-Smith, J. A.; Lavallee, D. K. *Bioconjugate Chem.* **1990**, *1* (5), 305–308.

(10) (a) Haensler, J.; Szoka, F. C., Jr. *Bioconjugate Chem.* **1993**, *4* (5), 372–379. (b) Wang, J.; Jiang, M.; Nilsen, T. W.; Getts, R. C. *J. Am. Chem. Soc.* **1998**, *120*, 8281–8282.

(11) (a) Kaifer, A. E. *Acc. Chem. Res.* **1999**, *32*, 62–71. (b) Venturi, M.; Serroni, S.; Juris, A.; Campagna, S.; Balzani, V. *Topics Curr. Chem.* **1998**, *197*, 194–226. (c) Schenning, A. P. H. J.; Martin, R. E.; Ito, M.; Diederich, F.; Boudon, C.; Gisselbrecht, J.; Gross, M. *Chem. Commun.* **1998**, 1013. (d) Hall, H. K., Jr.; Polis, D. W. *Polym. Bull.* **1987**, *17* (5), 409–416. (e) Xu, Z.; Moore, J. S. *Acta Polym.* **1994**, *45* (2), 83–87. (f) Fox, M. A.; Jones, W. E., Jr.; Watkins, D. M. *Chem. Eng. News* **1993**, *71*, 38–48.

in and out of the larger PAMAM dendrimers.²⁵ Moreover, the “dendritic box” model¹⁸ was proposed for entrapping Bengal Rose and *p*-nitrobenzoic acid guest molecules inside a poly-(propylenimine) dendrimer (PPI) using a L-phenylalanine capping derivative, where the guest molecules could only be removed from the host dendrimers when the surface groups are removed. It was also shown that the number of guest molecules entrapped was roughly proportional to the void space within the PPI dendrimers, supporting the “shell-like” conformation.

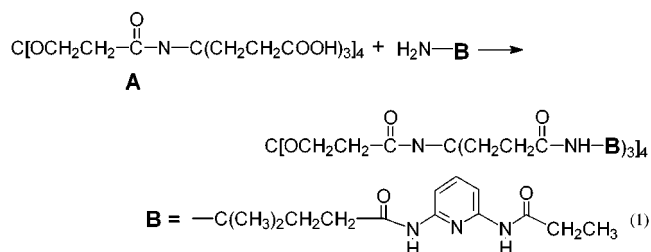
The “dense core” model has also been supported by several physical studies.¹⁹ The ¹³C and ²H relaxation properties of PAMAMs along with heteronuclear ¹³C–¹H NOE measurements²⁰ afford the average correlation times for the description of the segmental motions of protons in the interior and exterior regions. There was no anomalous suppression of functional group mobility for the ¹³C carbons located near the dendritic surface that would support the “dense shell” model. Only dense packing in the interior regions was noted as a significant gradual decrease in mobility of the interior chains in the dendrimers was observed. Recent studies of a dendrimer with a paramagnetic Fe₄S₄(SR)₄²⁻ core revealed significant decreases in *T*₁ values for protons located in both the interior and exterior regions, suggesting that the dendritic arms are folded back into the core.²¹ Since the efficiency of paramagnetic contribution to nuclear relaxation rates is a function of the distance between the resonating nucleus and the metal center (i.e., *T*₁ ∝ *r*_{M–H}⁶), the decrease in *T*₁ values reflects that the termini are close to the paramagnetic core. It should be noted that the ¹H NMR signals were not significantly hyperfine-shifted in this study.

An interconversion between the “dense shell” and the “dense core” models under different conditions has also been suggested. For example, a pH dependence of the hydrodynamic radii of acid terminated polyamido dendrimers has been demonstrated by means of NMR measurement of molecular diffusion.²² In these experiments, the “dense core” configuration is promoted at low pHs and is characterized by smaller hydrodynamic radii, whereas the hydrodynamic radii increase under neutral pH conditions supporting the larger “dense shell” configuration. The possibility of changing the size and shape of dendrimers by altering experimental conditions, such as temperature, salt concentration, and pH has also been noted.²³ A recent Monte Carlo computer simulation reveals that polyelectrolytic dendrimers should transform from a dense shell to a dense core configuration when the ionic strength of their solvents is increased.²⁴

The diamidopyridino dendrimers can be readily synthesized and have been previously examined for specific H-bonding to glutarimide and barbituric acid.⁷ The main advantages of using this dendrimer family for the investigation of structural features of dendrimers are (1) the diamidopyridino metal-binding site can be readily incorporated into many different dendritic loci for site specific structural analysis, and (2) the metal binding is quite kinetically labile, which permits the use of saturation transfer NMR techniques for the characterization of the metal-binding environment. We report herein NMR studies of several diamidopyridino-containing dendrimers with the metal-binding site near the core and surface of the macromolecules. These studies shed light on the mobility and cooperativity of the metal-binding dendritic arms. Flexibility in both the synthesis and structure of these dendrimers has facilitated the detailed study of their solution structure. Characterization and understanding of the internal microenvironment of dendrimers, as well as the location and mobility of the dendrimer end groups, are critical for further development of suitable applications.

Experiment Procedures

Chemicals and Sample Preparations. Dendrimers with internal diamidopyridino binding sites were synthesized according to previously published procedures.⁷ The schematic structures of a few dendrimers in this family are shown in Figure 1. The dendrimer with diamidopyridino binding sites near their surface was synthesized by coupling the alkylamine building block **B**-NH₂ to the terminal carboxylic acids of polyamido dendrimer **A** (eq 1) using standard peptide coupling conditions as previously reported.^{7,25} Two polyamido dendrimers with 12 and 36 2,6-diamidopyridino groups bound to the surface have been synthesized and characterized with 1D and 2D homo- and heteronuclear NMR and mass spectroscopies²⁵ (which will be reported elsewhere). The 12 and 36 “external diamidopyridino dendrimers” (MW = 4 465 and 13 464 Da, respectively) are soluble in MeOH and CH₂Cl₂.



All reagents were purchased from Sigma-Aldrich Chemical Co. (Milwaukee, WI). Cobalt(II) nitrate or chloride was titrated into the diamidopyridino dendrimers in either MeOH or MeCN to produce the paramagnetic Co(II)-dendrimer complexes for the ¹H NMR studies. The presence of 1/4 equiv of Co(II) per dendrimer affords a clean ¹H NMR spectrum, which represents the 1:1 Co(II)-dendrimer complex, devoid of complexes with multiple Co(II) binding to the dendrimer.

Nuclear Magnetic Resonance Experiments. ¹H NMR spectra were acquired on a Bruker AMX360 and a Bruker DRX250 spectrometers. Samples were prepared in CD₃OD, CD₃OH, CD₃CN, or other appropriate solvents. The ¹H NMR chemical shifts were referenced to an external TMS (tetramethylsilane) standard. The 1D ¹H NMR spectra of samples with upper mM concentration were acquired with 8 K data points, a 90° pulse, ≤800 transients, and a 150–500 ms recycle time. Either a Gaussian or an exponential window function was applied to the free induction decay (FID) prior to the Fourier transformation to improve the resolution or signal-to-noise ratio. The “super WEFT” pulse sequence²⁶ D₁-180°-D₂-90° was employed for acquiring spectra of samples prepared in CD₃OH, where D₁ and D₂ were short delay times which were appropriately adjusted to minimize the solvent CD₃OH signal.

(17) (a) Bauer, B. J.; Topp, A.; Prosa, T. J.; Amis, E. J.; Yin, R.; Qin, D.; Tomalia, D. A. *Polym. Mater. Sci. Eng.* **1997**, *77*, 87. (b) Amis, E. J.; Topp, A.; Bauer, B. J.; Tomalia, D. A. *Polym. Mater. Sci. Eng.* **1997**, *77*, 183. (c) Valachovic, D. E.; Bauer, B. J.; Amis, E. J.; Tomalia, D. A. *Polym. Mater. Sci. Eng.* **1997**, *77*, 230.

(18) (a) Jansen, J. F. G. A.; Meijer, E. W.; de Brabander-van den Berg, E. M. M. *J. Am. Chem. Soc.* **1995**, *117* (15), 4417–4418. (b) Jansen, J. F. G. A.; de Brabander-van den Berg, E. M. M.; Meijer, E. W. *Science* **1994**, *266*, 1226–1229.

(19) (a) Mansfield, M.; Klushin, L. *J. Phys. Chem.* **1992**, *25*, 4541. (b) Mourey, T. H.; Turner, S. R.; Rubinstein, M.; Frechet, J. J.; Hawker, C. J.; Wooley, K. L. *Macromolecules* **1992**, *25*, 2401. (c) Wooley, K. L.; Klug, C. A.; Tasaki, K.; Schaefer, J. J. *Am. Chem. Soc.* **1997**, *119*, 53.

(20) Meltzer, A.; Tirrell, D.; Jones, D.; Ingelfield, P.; Hedstrand, D.; Tomalia, D. *Macromolecules* **1992**, *25*, 4541.

(21) Gorman, G. B.; Hager, M. W.; Parkhurst, B. L.; Smith, J. C. *Macromolecules* **1998**, *31*, 815–822.

(22) Young, J. K.; Baker, G. R.; Newkome, G. R.; Morris, K. F.; Johnson, C. S. *Macromolecules* **1994**, *27*, 3464–3471.

(23) Briber, R.; Bauer, B.; Hammouda, B.; Tomalia, D. *Polym. Mater. Sci. Eng.* **1992**, *67*, 430.

(24) Welch, P.; Muthukumar, M. *Macromolecules* **1998**, *31*, 5892–5897.

(25) Epperson, J. D. Ph.D. Dissertation, University of South Florida, 1999.

(26) Inubushi, T.; Becker, E. D. *J. Magn. Reson.* **1983**, *51*, 128–133.

In the presence of chemical exchange, such as the binding of a paramagnetic metal ion to a ligand L to form a labile ML complex, $M + L \rightleftharpoons M-L$, NMR saturation transfer can occur between the paramagnetic M-L complex and its diamagnetic counterpart L. This can be studied with the saturation transfer techniques used for the detection of the nuclear Overhauser effect (NOE), such as 1D exchange difference spectroscopy²⁷ (with the decoupler set on and off the signal of interest) and the 2D EXSY²⁸ pulse sequence ($D_1-90^\circ-\tau_1-90^\circ-\tau_{mix}-FID$). The 1D difference spectra, presented here, were acquired with 8 K data points and processed with 0.3–10 Hz line broadening via exponential multiplication before Fourier transformation. The 2D EXSY spectra were acquired with 1 K \times 256 data points and a 20–50 ms mixing time, then zero-filled to 1 K \times 1 K data points, and with a 45–60° shifted sine-squared-bell window function applied in both dimensions prior to Fourier transformation, followed by baseline correction.

The 2D TOCSY and COSY spectra employed 2 K \times 512 data points for diamagnetic samples and 1 K \times 256 data points for paramagnetic samples. Several COSY spectra were acquired with 512 \times 128 data points to decrease the acquisition time and increase the number of scans for the detection of coherence transfer between/among the very broad hyperfine-shifted signals. The decoupler was used for solvent suppression for samples prepared in CD₃OH. A 45–60° shifted sine-squared-bell window function was applied to both dimensions prior to Fourier transformation and processed in phase-sensitive mode without symmetrization in TOCSY spectra. A 0°-shifted sine-squared-bell window function was applied to both dimensions in COSY spectra prior to Fourier transformation and processed in the magnitude mode and followed by symmetrization. Recycle times for 2D spectra were typically 150–250 ms for the paramagnetic Co(II)–dendrimer complexes.

Nonselective proton spin–lattice relaxation times (T_1) for all the Co(II)–dendrimer complexes were acquired by the use of the inversion–recovery method²⁹ ($D_1-180^\circ-\tau-90^\circ-FID$) with 16 different τ values and determined by a three-parameter fitting program on the spectrometer. Because the paramagnetic contribution to the nuclear relaxation times ($T_{1,M}$) in paramagnetic metal complexes is dependent upon the sixth power of the metal–nucleus distance (r_{M-H}), relative distances can be obtained with respect to a reference distance from a well-defined nucleus, i.e., $r_{M-H} = (T_{1M}/T_{1Mref})^{1/6} \times r_{M-Href}$. The meta proton on the rigid pyridine ring at 20.1 ppm ($T_1 = 39.1$ ms) was chosen as the reference proton. The reference distance of 5.08 Å was obtained by building a model of the metal-binding site of the Co(II)–2,6-diamidopyridine complex with the Co(II)–N bond set to be 2.0 Å on the Cerius² molecular modeling program (Molecular Simulations, San Diego, CA).

Results and Discussion

The paramagnetic metal ion Co(II) has been used, as an NMR probe, for the characterization of the structure and function of biomolecules and synthetic metal complexes because it has favorable NMR properties. The electron relaxation time of high spin Co(II) is approximately 10^{-11} – 10^{-12} s, resulting in relatively sharp paramagnetically shifted (also dubbed as isotropically or hyperfine-shifted) ¹H NMR signals.³⁰ Since broad overlapping ¹H NMR signals have hindered detailed analysis of the structures of dendrimers, the examination of the hyperfine-shifted ¹H signals observed for Co(II)-bound dendrimers offers a logical alternative and is discussed in this paper. Lanthanides such as Yb³⁺ and Dy³⁺ with shorter electron relaxation times of 10^{-12} to 10^{-13} s would have provided even

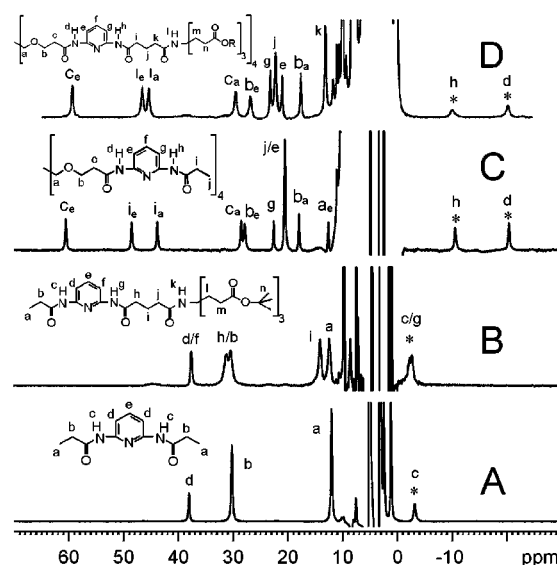


Figure 2. ¹H NMR spectra at 250.13 MHz of 2,6-diamidopyridino-containing molecules **1** (A), **2** (B), **9** (C), and **6** (D) in CD₃OD at 298 K. The dendrimers in (A) and (B) have 1 equiv of Co(II) added, and 1/4 equiv of Co(II) in (C) and (D). The asterisked signals are solvent exchangeable.

sharper signals; however, they did not bind to the diamidopyridino moieties of the dendrimers studied here. Nickel(II), which also possesses a favorable electron relaxation time of 10^{-10} to 10^{-12} s, was also examined, but it did not provide sharp isotropically shifted ¹H NMR signals for convenient study. The structures of different regions of a dendrimer can now be examined by selectively incorporating metal-binding sites into the macromolecule. For example, the internal cavities of a dendrimer can be examined by synthesizing a dendrimer with a metal binding site close to its core, while the incorporation of binding sites near the dendritic surface permits a structural analysis of the dendritic exterior.

A. Simple Amidopyridino Ligands as Models. Co(II) Complexes of *N*-(6-Propionylaminopyridin-2-yl)propionamide (1**).** The simple compound containing an amidopyridine moiety *N*-(6-propionylaminopyridin-2-yl)propionamide was prepared and characterized with NMR as described previously³¹ (Figure 2A). This molecule has the same metal binding site (i.e., a 2,6-diamidopyridino group) as all the dendrimers described in this report (Figure 1 and eq 1). Thus, the Co(II) complex of this small molecule is ideally suited as a model system for Co(II) complexes of those larger dendrimers. The formation of a 1-to-1 metal-to-ligand complex is conclusively established with a Job plot³² at 380 nm (Figure 3A), in which the maximum absorbance is observed at ligand mole fraction of 0.5, i.e., at Co(II):**1** = 1:1. This binding stoichiometry corroborates previous assignment based on chemical shifts of hyperfine-shifted ¹H

(27) Sanders, J. K. M.; Mersh, J. D. *Prog. Nucl. Magn. Reson. Spectrosc.* **1982**, *15*, 353–400.

(28) (a) Jeener, J.; Meiser, B. H.; Ernst, R. R. *J. Chem. Phys.* **1979**, *71*, 4546–4553. (b) Meier, B. H.; Ernst, R. R. *J. Am. Chem. Soc.* **1979**, *101*, 6441. (c) Boyd, J.; Brindle, K. M.; Campbell, I. D.; Radda, G. K. *J. Magn. Reson.* **1984**, *60*, 149–176.

(29) (a) Vold, R. L.; Waugh, J. S.; Klein, M. P.; Phelps, D. E. *J. Chem. Phys.* **1968**, *48*, 3831–3832. (b) Banci, L.; Luchinat, C. *Inorg. Chim. Acta* **1998**, *275–76*, 373–379.

(30) (a) Bertini, I.; Luchinat, C. *NMR of Paramagnetic Molecules in Biological Systems*; Benjamin/Cummings: Menlo Park, CA, 1986. (b) *NMR of Paramagnetic Molecules*; Berliner, L. J., Reuben, J., Eds.; Plenum: New York, 1993. (c) *NMR of Paramagnetic Molecules: Principles and Applications*; La Mar, G. N., Horrocks, W. D., Jr., Holm, R. H., Eds.; Academic: New York, 1973. (d) *Nuclear Magnetic Resonance of Paramagnetic Macromolecules*; La Mar, G. N., Ed.; NATO-ASI: Kluwer: Dordrecht, Netherlands, 1995. (e) Bertini, I.; Luchinat, C. *Coord. Chem. Rev.* **1996**, *150*. (f) Ming, L.-J. Nuclear Magnetic Resonance of Paramagnetic Metal Clusters in Synthetic Complexes and Proteins. In *Physical Methods in Bioinorganic Chemistry, Spectroscopy and Magnetism*; Que, L., Ed.; University Science Books: CA, 2000.

(31) Epperson, J. D.; Ming, L.-J.; Woosley, B. D.; Baker, G. R.; Newkome, G. R. *Inorg. Chem.* **1999**, *38*, 4498–4502.

(32) Polster, J.; Lachmann, H. *Spectrometric Titrations*; VCH: New York, 1989.

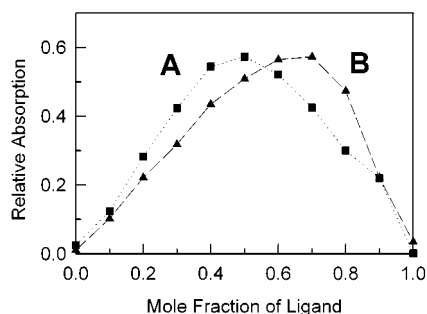


Figure 3. The Job plots (at 380 nm) that determine the stoichiometry of the Co(II) complexes of **1** (A) and **9** (B). A 1:1 complex is formed in A whereas a complex with Co(II)-to-dendritic arm ratio of 1-to-2 is formed in B.

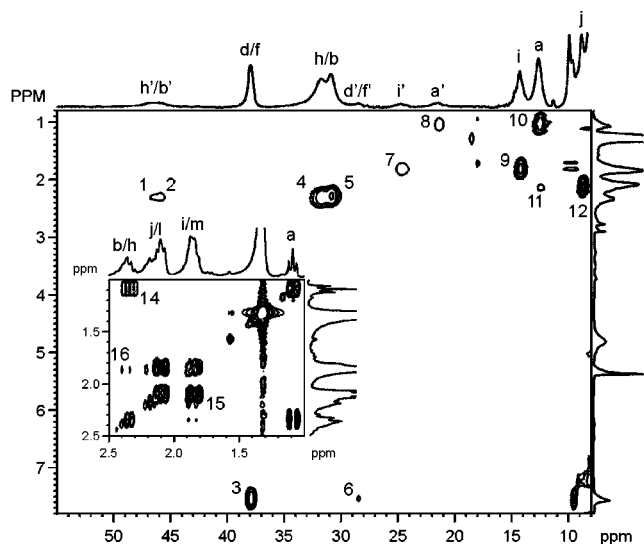


Figure 4. ^1H EXSY spectrum (250.13 MHz, 298 K, mixing time 30 ms, and a recycle time of 193 ms) of a 1:1 Co(II)-**2** complex in CD_3OD , which shows a correlation between the hyperfine-shifted signals of the Co(II) complex with the diamagnetic signals of the free ligand. The signals labeled with primes are due to a small amount of 1:2 Co(II)-**2** complex. The inset shows COSY identification of a few signals in the diamagnetic region.

NMR features of the complex. A 1:2 Co(II)-**1**₂ complex can be formed only in the presence of a large excess of **1** (>1200 equiv) which can be detected with an electrospray mass spectrometer ($[\text{M} + \text{H}]^+$, m/z 502.4). Three new hyperfine-shifted ^1H NMR signals appeared at 47.0 (methylene), 29.2 (methylene), and 23.1 (methyl) ppm in the 1:2 complex as indicated previously.³¹

***N*-(6-Aminotris(*tert*-butyl ester)glutrarlyaminopyridin-2-yl)propionamide (**2**) and Its Co(II) Complex.** This molecule represents a model for one of the four central arms of the 12-ester polyamido dendrimer with internal diamidopyridino binding sites discussed below. The Co(II) complexes of this molecule can also serve as models for the Co(II) complexes of those larger amidopyridino-containing dendrimers. The hyperfine-shifted ^1H NMR signals (Figure 2B) for the Co(II)-**2** complex can be assigned with a 2D EXSY experiment (Figure 4) as the complex undergoes chemical exchange with the free ligand **2** in solution; i.e., the signals at 32.4 and 31.5 ppm are assigned to the methylene C_6H_2 protons; 15.1 ppm, C_3H_2 protons; 13.2 ppm, methyl protons; 38 ppm, pyridine *m*-protons; and 8.8 ppm, C_3H_2 protons. It should be noted that the methylene and methyl signals and the pyridine ring protons of this complex have similar chemical shifts to the corresponding protons in the 1:1 Co(II)-**1**

complex (Figures 2A and B), suggesting the formation of a 1:1 Co(II)-**2** complex. Several smaller peaks are also observed for Co(II)-**2** at 47 (h'), 46.5 (b'), 28.5 (d'/f'), 25 (i'), and 22 (a') ppm (Figure 4) which are similar to those of Co(II)-**1**₂,³¹ consistent with a 1:2 Co(II)-**2** complex. This complex undergoes chemical exchange with the free ligand according to the equilibrium $\text{Co(II)-2}_2 \rightleftharpoons \text{Co(II)-2} + \text{2}$ as shown by the cross-peaks 1, 2, 6, 7, 8, and 11 in the EXSY spectrum.

B. Dendrimers with Internal Diamidopyridino Metal-Binding Sites. The ^1H and ^{13}C NMR spectra of the 12-, 36-, and 108-acid- (**3**, **4**, and **5** in Figure 1) and ester-terminated (**6**, **7**, and **8** in Figure 1) dendrimers in CDCl_3 and CD_3CN have been previously reported.⁶ The chemical shifts of the ^1H NMR signals changed slightly under the conditions employed here (in D_3COH and D_3COD) and can be easily assigned by comparing their 1D and 2D NMR spectra with those previously assigned.

^1H NMR Spectrum of 1:1 Co(II)-6**.** By adding 1/4 equiv of Co(II) to dendrimer **6**, a 1:1 Co(II):dendrimer complex is formed, and its ^1H NMR spectrum is presented in Figure 2D. In this case, only the dendrimer molecules which bind Co(II) would show hyperfine-shifted ^1H NMR signals, which have previously been fully assigned by the use of 1D and 2D (COSY, TOCSY, and EXSY) NMR techniques.³¹ Briefly, the signals at 59.4/29.5, 46.6/45.4, 26.7/17.5, 22.1, 11.6/9.14, and 12.9 ppm are assigned to the geminal $\text{c}_{e/a}$, $\text{i}_{e/a}$, $\text{b}_{e/a}$, j , $\text{a}_{e/a}$, and k protons, respectively; the signals at 23.1/20.1 and 1.4 ppm, the pyridine ring *meta*-protons and *para*-proton; the signals at -10.3 and -20.5, the solvent exchangeable 2,6-pyridinoamide NH protons of the Co(II)-bound arms; and the signals at 10.9 and 10.5 ppm, the 2,6-pyridinoamide NH protons of the two "proximal" noncoordinated dendritic arms. The other two arms not directly bound to the metal ion also exhibit significant isotropic shifts, since they are close to the metal-bound arms and gain significant isotropic shifts through the dipolar mechanism. The average chemical shifts of the geminal protons are very similar to those of the corresponding protons in Co(II)-**1**₂ and Co(II)-**2**₂, indicating the formation of complexes with one Co(II) bound to two dendritic arms.

^1H NMR Spectrum of a 1:1 Co(II)-Bound Tetrakisdiamidopyridino Dendrimer (9**).** For the purpose of a complete comparison, the dendrimer-mimicking tetrakisdiamidopyridine **9** was also prepared according to previous procedures³³ which does not possess the terminal "Behera's amine" building blocks (Figure 1). This compound represents a simple model for the joining of four *N*-(6-propionylaminopyridin-2-yl)propionamide ligands **1** to a four directional core. It is also instructive to compare the Co(II)-**9** complex to the Co(II)-**6** complex studied previously³¹ to see how the terminal *tert*-butyl esters of **6** affect the metal binding property and the coordination sphere.

The hyperfine-shifted ^1H NMR signals for the 1:1 Co(II)-**9** complex (Figure 2C) are fully assigned by the use of EXSY, TOCSY, and COSY techniques. The EXSY spectrum (Figure S1, Supporting Information) revealed cross-peaks between the hyperfine-shifted signals and their corresponding diamagnetic signals. For example, the signals at 63 (c_e) and 29 ppm (c_a) give cross-peaks to their diamagnetic counterparts at 2.4 ppm and cross-peaks to a signal corresponding to the same protons on the metal-free proximal arms of the complex (cross-peaks $\text{3}_{e/a}$ and $\text{3}'$, respectively). The rest of the hyperfine-shifted signals are assigned as shown in Figures S1. This complex display spectral features similar to those of Co(II)-**6** (Figure 2D), suggesting that the structure of the metal binding environment

(33) He, E., Ph.D. Dissertation, 1998, University of South Florida.

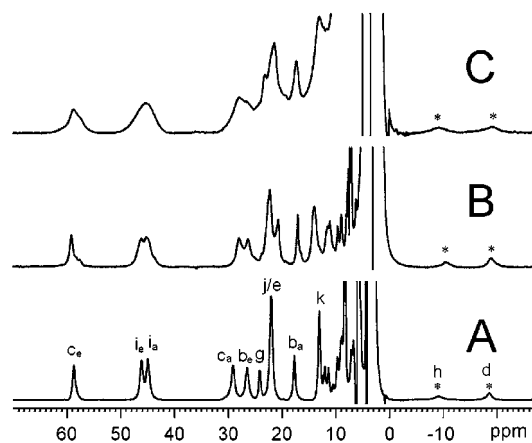


Figure 5. ^1H NMR spectra at 250.13 MHz of Co(II) complexes of **3** (A), **4** (B), and **5** (C) in CD_3OH and 25 $^\circ\text{C}$. The asterisked signals are solvent exchangeable. Broader signals are observed for the larger dendrimers as a result of an increase in the molecular size.

of the two complexes are quite similar. The most noticeable feature in the spectrum for the Co(II)–**9** complex is the presence of a large methyl signal at 21 ppm (signal j, Figure 2C). The chemical shift of this signal indicates that a 1-to-2 metal-to-dendritic arm complex is formed when compared to Co(II)–**1** and Co(II)–**2** complexes (Spectra A and B, Figure 2). Furthermore, the Job plot clearly shows a 1:2 ratio for the metal with respect to the dendritic arms, in which the maximum absorption occurs at mole fraction ratio of Co(II):dendritic arm = 1:2 (Figure 3B). To have a systematic view of this family of dendrimers, the Co(II) complexes of the 12-, 36-, and 108-acid diamidopyridino dendrimers have been further investigated and discussed below.

^1H NMR Spectrum of a Co(II)–12 Acid Diamidopyridino Dendrimer (3**).** By adding 1/4 equiv of Co(II) to dendrimer **3** (Figure 1) in D_3COD , a Co(II):dendrimer complex can be detected and its ^1H NMR spectrum is presented in Figure 5A. The overall spectral features of this complex are very similar to those of Co(II)–**6** and Co(II)–**9** (Figure 2), indicating the formation of a complex with Co(II) bound to two dendritic arms and that the removal of the terminal ester groups does not significantly affect the internal structure of the diamidopyridino dendrimer. No new hyperfine-shifted signals are detected, indicating the lack of binding of the terminal acid groups to the Co(II) ion. The 2D EXSY spectrum of this complex (Figure S2, Supporting Information) concludes its signal assignment, which is almost identical to that of Co(II)–**6**.³¹ As in the case of Co(II)–**9** discussed above, signals due to the metal-free arms of the complex are also slightly shifted in the EXSY spectrum due to their closeness to the metal bound by the other two arms of the same molecule.

^1H NMR Spectrum of a Co(II)–36 Acid Diamidopyridino Dendrimer (4**).** Upon the addition of 1/4 equiv of Co(II) to the 36-acid diamidopyridino dendrimer **4**, a Co(II)–**4** complex is formed, and its ^1H NMR spectrum is presented in Figure 5B. The spectrum is similar to those of Co(II)–**3** and Co(II)–**6** complexes (Figures 5A and 2D); however, the signals are broader for this complex, and some of the signals are partially overlapped, which prevented thorough investigation in our previous study.³¹ By appropriately choosing the acquisition parameters in the EXSY spectrum, chemical exchange cross-peaks can be detected between those of the complex and the free dendrimer which allow signal assignment to be completed (Figure 6). For example, the methylene protons $c_{e/a}$ on the Co(II)-bound dendritic arms are detected at 60.2 and 28.2 ppm,

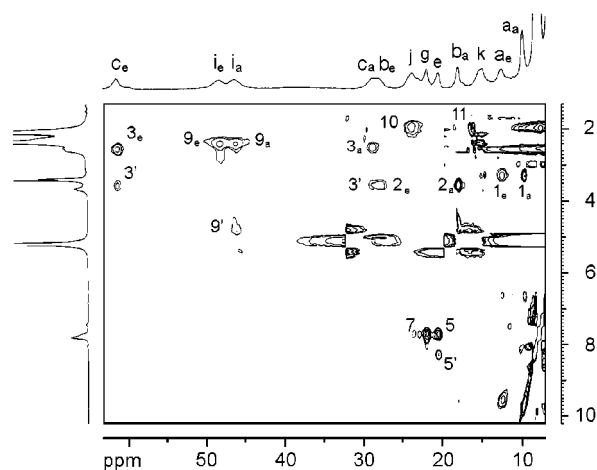


Figure 6. ^1H EXSY spectrum (250.13 MHz, 298 K, 1 K \times 256 data points, mixing time 20 ms, and a recycle time of 133 ms) of **4** in the presence of 1 equiv of Co(II) in CD_3OD . The primed labels are cross-peaks due to exchange counterparts on the proximal unbound dendritic arms.

which exhibit cross-peaks to their counterpart diamagnetic signal at 2.4 ppm (cross-peaks $3_e/3_a$ in Figure 6). They also show EXSY cross-peaks to a signal for the same protons on the proximal arm not bound to the Co(II) ion at 3.36 ppm (cross-peaks $3'$). Other signals can also be assigned accordingly as shown in the figure.

The short nuclear relaxation times and the small size of the complexes Co(II)–**9**, Co(II)–**3**, and Co(II)–**6** (MW = 742, 2162, and 2836 Da, respectively) discussed above precluded the use of the NOE techniques for a more detailed structural analysis of these dendrimers because NOE intensity in paramagnetic macromolecules is proportional to the rotational correlation time and inversely proportional to the nuclear relaxation rates.³⁴ Therefore, only larger Co(II)–dendrimers, such as Co(II)–**4**, can be potentially studied by the use of the NOE techniques, which was also demonstrated in our previous study on Co(II)–**7** complex.³¹ The axial and equatorial configurations of the $-\text{C}_b\text{H}_2-\text{C}_c\text{H}_2-$ protons in Co(II)–**4** have been fully established based on NOE interactions (Figure 7), in which only the equatorial proton pair (c_e and b_e) exhibit significant NOEs (Figure 7A), but not the axial–equatorial pair (c_e and b_a). However, no clear NOE is observed between protons i and j (Figure 7B), which may be caused by the faster local motion of these protons located farther from the rigid core than protons b and c. Since j has a longer relaxation time (21.2 ms) than that of b_a (14.5 ms) at 293 K, it should exhibit more intense NOE signal than b_a if their rotational correlation times are the same.^{30,34} However, we observed the opposite which indicates a faster motion of j than the “inner proton” b_a .

^1H NMR Spectrum of a 1:1 Co(II)–108 Acid Diamidopyridino Dendrimer (5**).** By the addition of small amounts of Co(II) (<1/4 equiv per dendrimer) to the much bigger dendrimer **5** (see structure in Figure 1), a 1:1 Co(II):dendrimer complex is formed, and its ^1H NMR spectrum is presented in Figure 5C. The hyperfine-shifted ^1H NMR signals for this complex are much broader than those of the Co(II) complexes of the 12- and 36-acid dendrimers (Figures 5A and 5B); however, two adjacent geminal pairs can still be identified (i.e., the cross-peaks 1 and 3 for the pairs and the peak 2 between these adjacent

(34) (a) Neuhaus, D.; Williamson, M. P. *The Nuclear Overhauser Effect in Structural and Conformational Analysis*; VCH: New York, 1989. (b) Noggle, J. H.; Schirmer, R. E. *The Nuclear Overhauser Effect*; Academic: New York, 1971.

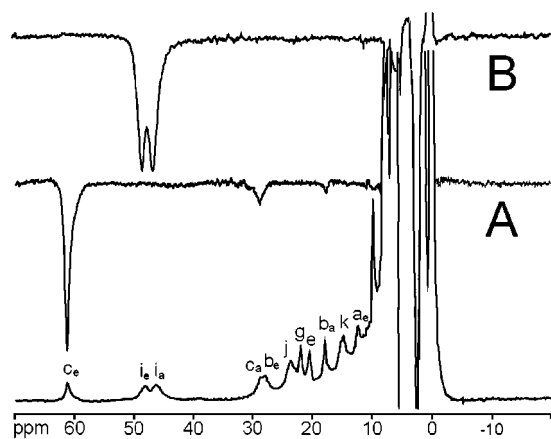


Figure 7. ^1H NMR spectrum (250.13 MHz) of **4** in the presence of 1 equiv of Co(II) in CD_3OD at 293 K, and the 1D NOE difference spectra of the complex with the 61.2 ppm signals (A) and the partially overlapped signals at 48 and 46 ppm (B) saturated for 50 ms. Cross relaxation between protons *i* and *j* is barely seen.

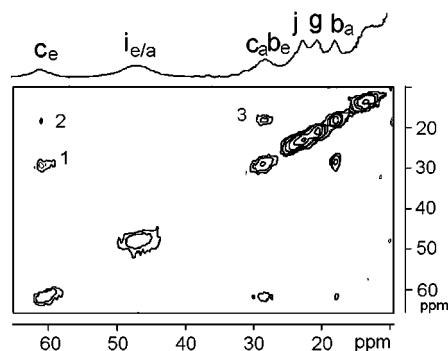


Figure 8. ^1H NOESY spectrum (250.13 MHz, 298 K, $1\text{ K} \times 256$ data points, mixing time 30 ms, and a recycle time of 243 ms) of Co(II)-**5** in CD_3OD .

pairs in Figure 8). The similar chemical shifts of the Co(II) complexes of **3**, **4**, **5**, **6**, and **9** suggest that the internal structures of these dendrimer do not change significantly and that complexation to metal ions (or guest molecules) may occur in these dendrimers in the same manner, despite their dramatically different sizes. The lack of vicinal NOE interaction between *i* and *j* suggests that these protons may still have a large degree of freedom that affords significant local motion to decrease the NOE. This NOE detection revises the previous assignment of the two magnetically inequivalent C_6H_2 protons.

C. Co(II)-Complexes of Dendrimers with External Diamidopyridino Binding Sites. ^1H NMR Spectrum of a Co(II)-12 External Diamidopyridino Dendrimer (10). Co(II) was found to bind to **10** possessing 12 2,6-diamidopyridino sites (structure in Figure 9) which affords a ^1H NMR spectrum in Figure 9 (top trace); however, the exact metal-to-ligand stoichiometry could not be determined by the Job plot. Nevertheless, a mixture of two species was observed by comparing their ^1H NMR spectral features with those of the Co(II) complexes of **3**–**6** as discussed above. The signals can be fully assigned with an EXSY experiment as indicated in Figure 9. The overall spectral features of the major species resemble those of Co(II)-**1** and Co(II)-**2** complexes (Figure 2B), which reflects the formation of a complex with Co(II) bound to only one dendritic arm. However, the binding of Co(II) to two dendritic arms is more prevalent in **10** (primed labels) than in **1** and **2**. The presence of chemical exchange among the two complexes and the metal-free form may have contributed to signal broadening

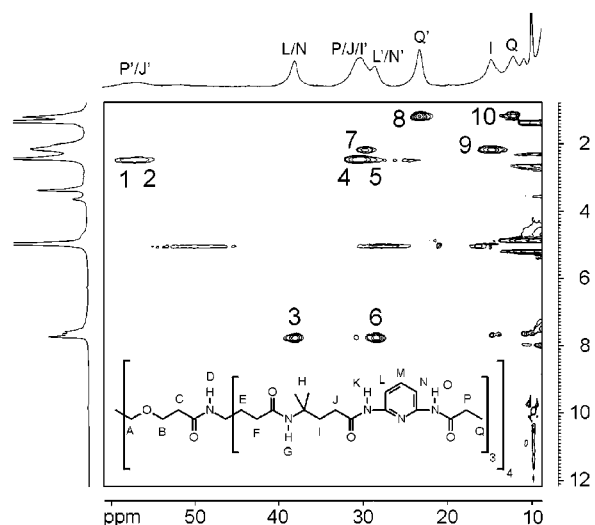


Figure 9. $^1\text{EXSY}$ spectrum (250.13 MHz, 298 K, $1\text{ K} \times 256$ data points, mixing time 20 ms, and a recycle time of 133 ms) of **10** in the presence of 1 equiv of Co(II) in CD_3OD . The signals at 24 and 13 ppm show cross-peaks to the same diamagnetic signal at 1.3 ppm (cross-peaks 8 and 10) assigned to the terminal methyl protons (Q). Two sets of signals are also present for other protons for the complexes with Co(II):dendritic arm ratios of 1:1 and 1:2, as observed in the Co(II) complexes of **2** (Figure 4).

when compared with the signals of Co(II)-**3** of a similar molecular size.

It is important to note that all of the methylene geminal protons in this sample are magnetically equivalent and show only single peaks in contrast to the Co(II) complexes of the dendrimers with internal diamidopyridino binding sites (**3**–**8**). This observation indicates that a greater degree of rotational freedom is present in the external portions (surface) of the dendrimer than in the inner regions (core). Furthermore, in contrast to **3**–**8** which possess internal diamidopyridino and bind Co(II) with two of their dendritic arms with a great cooperativity and those small ligands **1** and **2** which preferentially forms 1:1 metal:ligand complexes and lack ligand binding cooperativity, complexes with Co(II) bound to both one and two dendritic arms are clearly observed for **10**. This observation indicates that ligand binding cooperativity of the functional groups on the dendritic arms becomes smaller when they are farther away from the core, which provides a hint for future synthesis of functional dendrimers when cooperativity is needed between/among the dendritic arms.

D. Co(II) Titration to 12-Ester Diamidopyridino Dendrimer 6. Titration in Methanol. The titration of Co(II) to dendrimer **6** in MeOH is presented in Figure S3 in the Supporting Information. Upon addition of 1/4 equiv of Co(II) (i.e., $[\text{Co}]/[\text{dendrimer}] = 1/4$), several hyperfine-shifted signals can be clearly detected in the spectral region of 60 to -25 ppm (Figure 2D). At this Co(II) concentration, there is at most only one Co(II) bound per dendrimer molecule. When 1 equiv of Co(II) is reached, several new signals begin to appear, such as the two weak signals at 61 and 58 ppm. This suggests that some dendrimer molecules bind one Co(II) ion, and some may bind two Co(II) ions. It is important to note that the chemical shifts of the hyperfine-shifted ^1H NMR signals are still comparable to those of the 1:2 complex Co(II):**12**, consistent with each Co(II) binding to two dendritic arms of **6**.

By the time 4 equiv of Co(II) are added, several new hyperfine-shifted signals appear including two signals at 38 and 38.5 ppm and two solvent exchangeable signals in the upfield

region (marked with arrows, Figure S3). The two downfield signals give saturation transfer peaks to the aromatic pyridine signal at 7.64 ppm, indicating that they are the pyridine ring meta protons. The chemical shifts of these signals are consistent with the 1:1 Co(II):1 complexes for pyridine ring meta protons (signal d, Figure 2A). This result indicates that a greater amount of Co(II) is bound to only one dendritic arm at higher Co(II) concentrations, which overcomes binding cooperativity of dendritic arms. However, the 1:2 Co(II)–dendritic arm complex is still prevalent even in the presence of 4 equiv of Co(II) per dendrimer molecule, indicating a great metal binding cooperativity of the dendritic arms.

Titration in Acetonitrile. The titration of Co(II) to **6** in MeCN is presented in Figure S4, Supporting Information. Unlike the titration in MeOH described above, a “clean” spectrum is observed even when 4 equiv of Co(II) have been added. New signals corresponding to the complex with one Co(II) binding to only one dendritic arm do not appear until a large excess amount of Co(II) has been added, e.g., the weak signal at ~38 ppm with 100 equiv of Co(II) introduced. This result suggests that MeCN hinders the binding of Co(II) to only one dendritic arm, that lead to an apparently simultaneous binding of two dendritic arms to one Co(II) to exhibit a nearly complete cooperative binding. This observation also indicates that solvent has to be taken into consideration in future studies of the binding properties of metal ions and guest molecules with dendrimers.

^1H NMR Spectrum of Co(II)₂–6**.** By adding excess Co(II) (~20 equiv) to **6** in MeCN, a 2:1 Co(II)₂–dendrimer complex is partially formed (Figure S4), wherein two Co(II) ions are bound to four dendritic arms. The newly appeared signals at 27 and 18 ppm can be assigned to Co(II)₂–**6**, and serve as the initial point for the assignment of other signals as shown in Figure 10 (labeled with a prefix “2”). The chemical shift values of the isotropically shifted ^1H NMR signals are consistent with the binding of one Co(II) to two dendritic arms as observed in the spectra of the complexes Co(II)–**1**₂ and Co(II)–**2**₂ (Figure 2).³¹ A complete signal assignment of Co(II)₂–**6** can be achieved by the use of EXSY and COSY techniques (Figure 10), whereas the assignment of the signals due to the 1:1 Co(II)–**6** complex (labeled with a prefix “1”) is similar to those of Co(II)–**3** and Co(II)–**9**. Although much less shifted, the signals of the C_aH₂ protons exhibit quite different chemical shifts (Figure S5) due to two different orientations, axial-like and equatorial-like, which reflects the rigidity of the moieties near the core of the dendrimer. No exchange peaks are detected between the hyperfine-shifted signals and the signals of free dendrimer. This is expected since an excess amount of Co(II) has been added to the sample; thus, all dendrimer molecules should presumably have at least one Co(II) bound.

E. Effects of Temperature on Co(II)–6** Complex.** The ^1H NMR spectrum of Co(II)–**6** complex has been examined at different temperatures (Figure S6). A plot of the chemical shifts of the hyperfine-shifted signals versus $1/T$ (Figure S7) shows that most of the hyperfine-shifted signals move away from the diamagnetic region at lower temperatures in a linear fashion. For example, the inner C_aH₂COPy equatorial proton (c_e) shifts from 51 to 78 ppm when the temperature is lowered from 328 to 248 K. Likewise, the upfield solvent-exchangeable signals h and d at –7 and –15 ppm (barely detected at 328 K due to fast chemical exchange with the solvent) shift upfield to –15 and –29 ppm at 258 K, respectively. Moreover, an upfield hyperfine-shifted signal at –5 ppm is clearly observed at 248 K, corresponding to the para proton of the pyridine ring, which is buried in the diamagnetic region at 25 °C.

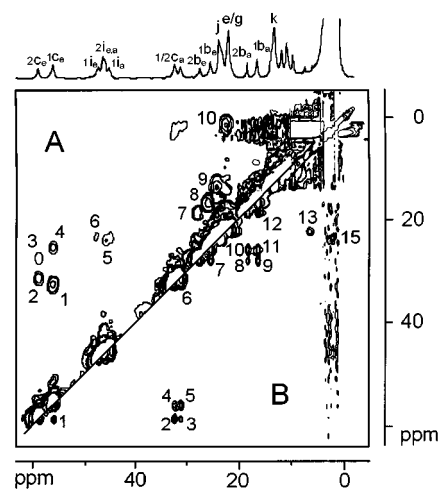


Figure 10. (A) ^1H COSY spectrum (250.13 MHz, 298 K, $1\text{ K} \times 256$ data points, 6 ms acquisition time, and a recycle time of 156 ms) and (B) ^1H EXSY spectrum (250.13 MHz, 298 K, $1\text{ K} \times 256$ data points, mixing time 30 ms, and a recycle time of 243 ms) of Co(II)–**6** (labeled with prefix “1”) and Co(II)₂–**6** (labeled with “2”) in CD₃CN. The two new signals at 18 and 27 ppm can be clearly assigned to 2b_{e/a}, which show COSY cross-peak 7 to each other and to adjacent 2c_e with anti configuration (peak 3). COSY cross-peaks between 1/2c_e and their adjacent methylene protons 1/2b_e are detected (3 and 4 in A). The latter signals in turn show cross-peaks to their respective geminal partners (1/2b_a) in EXSY (8 and 11 in A) and COSY spectra (7 and 8 in B). The inner methylene C_aH₂ protons signals of Co(II)₂–**6** can also be assigned to be at 13, 11.7, and 9.6 ppm in the EXSY spectrum (cross-peaks 2–4, Figure S4 in Supporting Information). The hyperfine-shifted signals of both sets of Co(II)-coordinated dendritic arms are overlapped at 22 ppm for the pyridine ring meta protons (1 and 2e/g). A COSY cross-peak is noted between the signals at 22 and 1.5 ppm (peak 10), corresponding to the para proton on the pyridine ring. The COSY spectrum also reveals cross-peaks among the three pairs of adjacent methylenes further away from the core, i.e., 1i_{e/a}, 2i_{e/a}, 1/2j, and 1/2k (5, 6, and 9 in B) for both 1:1 and 2:1 complexes. Three upfield solvent exchangeable ^1H NMR signals at –12.8, –13.4, and –19.7 ppm are detected that correspond to the labile 2,6-pyridinoamido NH protons. The outer methylene (m/n) and methyl protons (o) cannot be clearly detected.

The signals corresponding to the outer PyrCOC₄H₂ geminal protons (i_{e/a}) at 61 and 64 ppm at 248 K collapse into one signal at 38 ppm when the temperature is raised to greater than 318 K. The core geminal protons including a_{e/a}, b_{e/a}, and c_{e/a}, however, do not collapse into one signal even at 328 K. These results imply that a much larger degree of rotational freedom with respect to the NMR time scale is present for the outer regions of the Co(II) complex of this dendrimer.

The T_1 values of the hyperfine-shifted signals for the Co(II) complexes of **3**, **4**, and **5** have been measured at different temperatures to assess the relative flexibility of a dendrimer in solution and how its conformational manifold might change with temperature. The T_1 values of all the protons in the three dendrimers generally increased with temperature (Figure 11), indicating that the dendrimers are in the “liquidlike” regime with short correlation times.^{21,35} However, the T_1 values of the larger 108-acid dendrimer show a smaller increase than those of the smaller 12-acid dendrimer, indicating the larger dendrimer is less “liquidlike” than the small ones. This liquidlike relaxation supports a more loosely packed “shell-like” structure¹⁴ of these complexes with their arms stretched out into the solution.

(35) (a) Bovey, G. A.; Jelinski, L.; Mirau, P. A. *Nuclear Magnetic Resonance Spectroscopy*, 2nd ed.; Academic Press: New York, 1988; Chapter 5. (b) Abragam, A. *The Principles of Nuclear Magnetism*, reprinted ed.; Oxford University Press: London, 1983; Chapter 8.

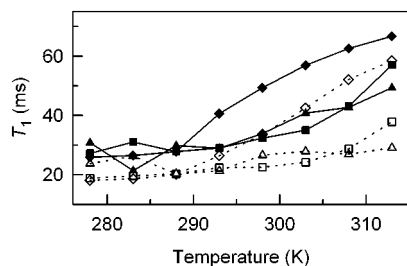


Figure 11. T_1 values for signals c_e (solid lines) and $i_{e/a}$ (dotted lines) for the Co(II) complexes of **3** (◆ and ◇), **4** (■ and □), and **5** (▲ and △) at different temperatures.

Table 1. Calculated Cross-Relaxation Rates (σ_{ij}), Rotational Correlation Times (τ_r), Intrinsic Relaxation Rates (ρ_i), and Hydrodynamic Radii (r) for 12-, 36-, and 108-Acid Terminated Tetrapyrindine Polyamido Dendrimers

	ρ_i (s^{-1})	σ_{ij} (s^{-1})	τ_r (s)	r (Å)
Co(II)- 3	14.31	-0.586	5.84×10^{-9}	18.6
Co(II)- 4	17.31	-2.42	1.11×10^{-8}	23.0
Co(II)- 5	22.19	-6.62	2.54×10^{-8}	30.4

F. Estimating the Size of a Dendrimer in Solution. The Co(II) complexes of the three dendrimers **3**, **4**, and **5** exhibit NOEs between nearby hydrogen atoms in MeOH at 273 K. In particular, clear NOEs can be observed between the pyridine para proton at -0.4 ppm to the two nonequivalent pyridine meta protons at 22 and 20 ppm. Since the distance between the meta and para protons is fixed (calculated to be 2.44 Å),³⁶ the hydrodynamic radii of the Co(II) complexes of the dendrimers can be estimated from the NOE intensity with respect to irradiation time described below.

The relative NOE is obtained as $\text{NOE}\% = [I(t) - I_0]/I_0$, where I_0 and $I(t)$ are the magnetizations of spin i without and with perturbation, respectively, of spin j for a period of time t . The cross relaxation rate and the intrinsic relaxation rate of i , ρ_i , in paramagnetic species with fast electron relaxation rates can be obtained by fitting NOE% with respect to t according to eq 2.^{30,34}

$$\text{NOE}\% = (\sigma_{ij}/\rho_i)[1 - \exp(-\rho_i t)] \quad (2)$$

The rotational correlation time, τ_r , can be calculated by solving eq 3,^{30,34}

$$\sigma_{ij} = \left(\frac{\mu_0 \gamma^2 \hbar}{4\pi}\right)^2 \frac{1}{10r_{ij}^6} \left(\frac{6\tau_r}{1 + 4\omega^2 \tau_r^2} - \tau_r\right) \quad (3)$$

where r_{ij} is the distance between the para and meta protons of the pyridine ring (2.44 Å) and other terms are physical constants as normally defined. The values of σ_{ij} , ρ_i , and τ_r obtained for the three Co(II)-dendrimer complexes are shown in Table 1.

The τ_r value obtained from eq 3 can be used in the Stokes-Einstein equation (eq 4) to yield the hydrodynamic radius a of the molecule under investigation,^{30,34}

$$\tau_r = 4\pi a^3 \xi / 3kT \quad (4)$$

where ξ is the solvent viscosity at temperature T (0.00082 J s m^{-3} at 273 K), and k is the Boltzmann constant. The a values of 18.6, 23.0, and 30.4 Å are obtained for the Co(II) complexes of **3**, **4**, and **5** (Table 1).

These hydrodynamic radii are ~ 10 – 12 Å larger than those values previously reported for the analogous 12, 36, and 108 acid-terminated polyamido dendrimers under acidic pHs, and 6–7 Å larger than those corresponding dendrimers under neutral pH conditions.²² For example, the reported hydrodynamic radii for the 12, 36, and 108 acid-terminated polyamido dendrimers at pH 3.5 are 8.24, 11.4, and 17.3 Å, respectively.²² The larger values noted for the Co(II) complexes of **3**, **4**, and **5** are indeed in agreement with those of the polyamido dendrimers reported previously, as the latter do not possess the internal extended 2,6-diamidopyridino binding sites or the $-\text{CH}_2\text{CH}_2\text{CH}_2-$ spacer arms, thus would be ~ 10 Å smaller. Furthermore, the smaller 6–7 Å increase for **3**, **4**, and **5** when compared with the polyamido dendrimers under neutral conditions²² suggests that the arms of the Co(II) complexes of the dendrimers studied here may not be fully extended in solution, which may be attributed to restriction in rotational freedom upon Co(II) binding or/and a “tight packing” of the arms in organic solvent due to the lack of charge repulsion.

Conclusion and Perspectives

The size, structure, and accessibility of the internal cavities of a dendrimer can determine, in part, its optimal host-guest interactions for catalysis, self-assembly, and molecular recognition and encapsulation. Indeed, the large size, spherical shape, and specific host-guest chemistry associated with many dendrimers have led researchers to suggest that they loosely mimic the structure and function of globular proteins.^{1b} Unlike proteins, however, dendrimers have not been successfully analyzed by means of X-ray crystallography due to their fractal nature.³⁷ Dendrimers also exhibit broad overlapping ^1H NMR spectral features, which further hinders their conformational analyses. Therefore, examination of the hyperfine-shifted ^1H NMR signals offers a logical alternative to probe this interesting interior environment of dendrimers.

There are some interesting properties about dendrimers revealed in our studies: (a) When the metal-binding 2,6-diamidopyridino moiety is placed into a dendrimer either on the surface or near the core, it is bound to Co(II) predominately with two dendritic arms per metal (although it is less pronounced in the former case). In other words, “cooperativity”, a unique property of many functional macromolecules, among the dendritic arms seems to be present in dendrimers that is not observed in simple ligands. (b) The configuration of the metal-binding site, which can potentially be built as an active site, is not affected by the size of the molecule on the basis of the similar NMR spectra. (c) A smaller degree of rotational freedom is demonstrated for the methylene groups close to the dendritic core as compared to the surface moieties for dendrimers with internal diamidopyridino metal binding sites. (d) No hyperfine-shifted ^1H NMR signals corresponding to the terminal methyl or methylene groups are detected for the Co(II) complexes of dendrimers **3**, **4**, and **5**, suggesting a “shell-like” conformation with their arms radiating out away from the core. (e) All of the T_1 values generally increased when the temperature is raised, indicating a “liquidlike” regime for these dendrimers of “shell-like” configuration. Only a “solidlike” regime with the T_1 values decreasing with increasing temperature would support the “dense core” model. (f) The calculated hydrodynamic radii of the Co(II) complexes of **3**, **4**, and **5** indicated that the arms of these dendrimers are extended in solution to nearly a full extent. The 3D model of the Co(II)-**3** built using the T_1 values of the

(36) Cerius², version 3.5; Molecular Simulations, Inc.: San Diego, CA.

(37) Ottaviani, M. F.; Bossmann, S.; Turro, N. J.; Tomalia, D. A. J. Am. Chem. Soc. **1994**, *116*, 661–671.

assigned hyperfine-shifted signals reported previously³¹ showed that the four pyridine rings of Co(II)-**3** are quite close to each other (≤ 6 Å) indicating a possible loosely packed interior that may be controlled by the Co(II) binding. Therefore, the data indicate that the structures of the metal (and possibly guest molecule) complexes of dendrimers with internal diamidopyridino moieties may lie closer to the "shell-like" model than the "dense core" model, which may be further controlled by the surface charge of the molecule and the solution conditions.

Paramagnetic metal ions have been extensively used as NMR probes over the past two decades for structural and mechanistic studies of biologically important macromolecules such as metalloproteins and metalloantibiotics;³⁰ however, they have not been widely applied to the study of other macromolecular systems. Systematic variation of the metal binding environment in different dendrimer frameworks and structure-based rational design of metallodendrimers for specific applications, such as

catalysis and molecule recognition, are expected to be forthcoming. In this paper, we report the use of paramagnetic Co(II) as an NMR probe for detailed characterization of a few dendrimers, which points a new direction for the application of NMR spectroscopy to the study of this unique family of synthetic macromolecules.

Acknowledgment. G.R.N. wishes to thank NSF (DMR-96-22609, DMR-99-01393) and the Office of Naval Research (N00014-99-1-0082) for support of this project.

Supporting Information Available: ¹H EXSY spectra of the Co(II) complexes of **3**, **6**, and **9** (3 spectra), ¹H NMR spectra of **6** upon Co(II) titration (2 figures), and temperature-dependent spectral change (2 figures). These materials are available free of charge via the Internet at <http://pubs.acs.org>.

JA015856Y